J Biomol NMR (2014) 60:283–288
DOI 10.1007/s10858-014-9874-7

NMR STRUCTURE NOTE

Long-chain flavodoxin FldB from *Escherichia coli*

Qian Ye · Wenyu Fu · Yunfei Hu · Changwen Jin

Received: 17 August 2014 / Accepted: 4 November 2014 / Published online: 8 November 2014

Biological context

Flavodoxins are a family of small electron transferases widely distributed in prokaryotes. They utilize a non-covalently bound flavin mononucleotide (FMN) molecule as the redox center, and are able to switch between three different redox states, namely the oxidized (ox) state, the one-electron reduced semiquinone (sq) state, and the two-electron reduced hydroquinone (hq) state (Knight and Hardy 1967). Since flavodoxins display two redox potentials and can transfer either one or two electrons at a time, they are functionally versatile. Flavodoxins have been identified to play important roles in various biological processes, including photosynthesis, methionine synthesis, biotin synthesis, and the activation of important enzymes such as pyruvate-formate lyase and ribonucleotide reductase (Sancho 2006). In eukaryotes, flavodoxins are integrated into multi-domain proteins and carry out similar redox functions.

Flavodoxins can be further classified into the long-chain and short-chain subfamilies, which are distinguished based on the presence or absence of a 20-amino acid extra segment. The flavodoxin-like domains in eukaryotic multi-domain proteins are more closely related to the short-chain subfamily. Previous investigations on the extra sequence suggested it is not directly involved in cofactor binding but may play a role in protein partner recognition and interactions, and it was proposed that the short-chain may derive from the long-chain group during evolution (López-Llano et al. 2004a, b). However, the underlying molecular mechanism is yet unclear and the structural determinants for the distinct biological functions of different flavodoxins remain elusive.

The *Escherichia coli* genome harbors several genes encoding flavodoxin proteins. Among them, the *fldA* gene encodes the well-characterized flavodoxin 1 protein which belongs to the long-chain subfamily and is essential for bacteria survival (Gaudu and Weiss 2000). The *fldB* gene encodes another long-chain flavodoxin which shares over 40 % sequence identity with FldA yet is functionally distinct. Insertion mutation of the *fldB* gene is not lethal to *E. coli*, and over expression of FldB could not substitute FldA (Gaudu and Weiss 2000). Evidence suggested that the *fldB* gene is a member of the superoxide response *soxRS* regulon, and its expression level was induced by paraquat (methyl viologen) (Gaudu and Weiss 2000). However, the exact function of FldB protein remains unclear.

We have previously carried out structural and dynamic studies of *E. coli* flavodoxins including the short-chain MioC and YqcA proteins as well as the long-chain FldA by solution NMR spectroscopy (Hu et al. 2006; Ye et al. 2014). The FldA protein exhibit global conformational exchanges without the presence of FMN cofactor, rendering one third of its backbone amide signals missing in the NMR spectra, and we were unable to determine its solution structures in the apo-form. In contrast, the FldB protein

Q. Ye · W. Fu · Y. Hu (✉) · C. Jin (✉)
Beijing Nuclear Magnetic Resonance Center, Peking University, Beijing 100871, China
e-mail: yunfei@pku.edu.cn

C. Jin
e-mail: changwen@pku.edu.cn

Q. Ye · C. Jin
College of Life Sciences, Peking University, Beijing 100871, China

Y. Hu · C. Jin
College of Chemistry and Molecular Engineering, Peking University, Beijing 100871, China

display relatively nice spectral properties in both the apo- and holo-states, thus providing a chance of obtaining high resolution structures of a long-chain flavodoxin in the presence or absence of the cofactor. Herein, we report the NMR structures of *E. coli* FldB protein in apo- and holo-forms, which provide insightful information for cofactor binding and electron transfer.

Methods and results

Protein expression and sample preparation

The *E. coli fldB* gene was cloned into the pET 21a (+) (Novagen) vector and expressed in *E. coli* BL21 (DE3) strain (Invitrogen). The cells were grown in 1 L Luria–Bertani (LB) broth medium containing 50 mg/mL of ampicillin at 35 °C. When the OD_{600} reached 0.8, the culture was centrifuged at 4 °C and resuspended in 250 ml of M9 minimal medium with ampicillin (Marley et al. 2001). After shaking at 35 °C for an hour, isopropyl-β-D-thiogalactoside (IPTG) was added to a final concentration of 0.4 mM to induce protein expression. The cells were harvested 8 h later and the protein was purified by anion-exchange chromatography (Mono Q) followed by a gel filtration (Superdex-75) with ÄKTA FPLC system (Amersham Biosciences). For preparations of $^{13}C/^{15}N$-labeled samples, $^{15}NH_4Cl$ and $^{3}C_6$-glucose were used in the M9 minimal medium.

For preparation of apo-FldB sample, the purified protein was precipitated using 5 % trichloroacetic acid (Edmondson and Tollin 1971). The supernatant containing the FMN molecule was removed and the precipitant was washed and refolded in a buffer containing 30 mM sodium phosphate (pH 7.0), 30 mM NaCl, and 20 mM dithiothreitol (DTT). The procedure was repeated several times to completely remove the FMN molecule. The holo-FldB sample was prepared by addition of excess FMN molecule. D_2O (5 %) was added into the NMR samples, and 2,2-dimethyl-2-silapentanesulfonic acid (DSS) was added as the internal chemical shift reference.

NMR spectroscopy and chemical shift assignments

NMR spectra were acquired at 25 °C on Bruker Avance 600 and 800 MHz spectrometers, both equipped with four RF channels and a triple-resonance cryo-probe with pulsed field gradients. Two-dimensional (2D) ^{15}N-edited heteronuclear single quantum coherence (HSQC) spectroscopy, three-dimensional (3D) HNCA, HNCACB, CBCA(-CO)NH, HNCO, HN(CA)CO, HBHA(CO)NH, (H)CCH-

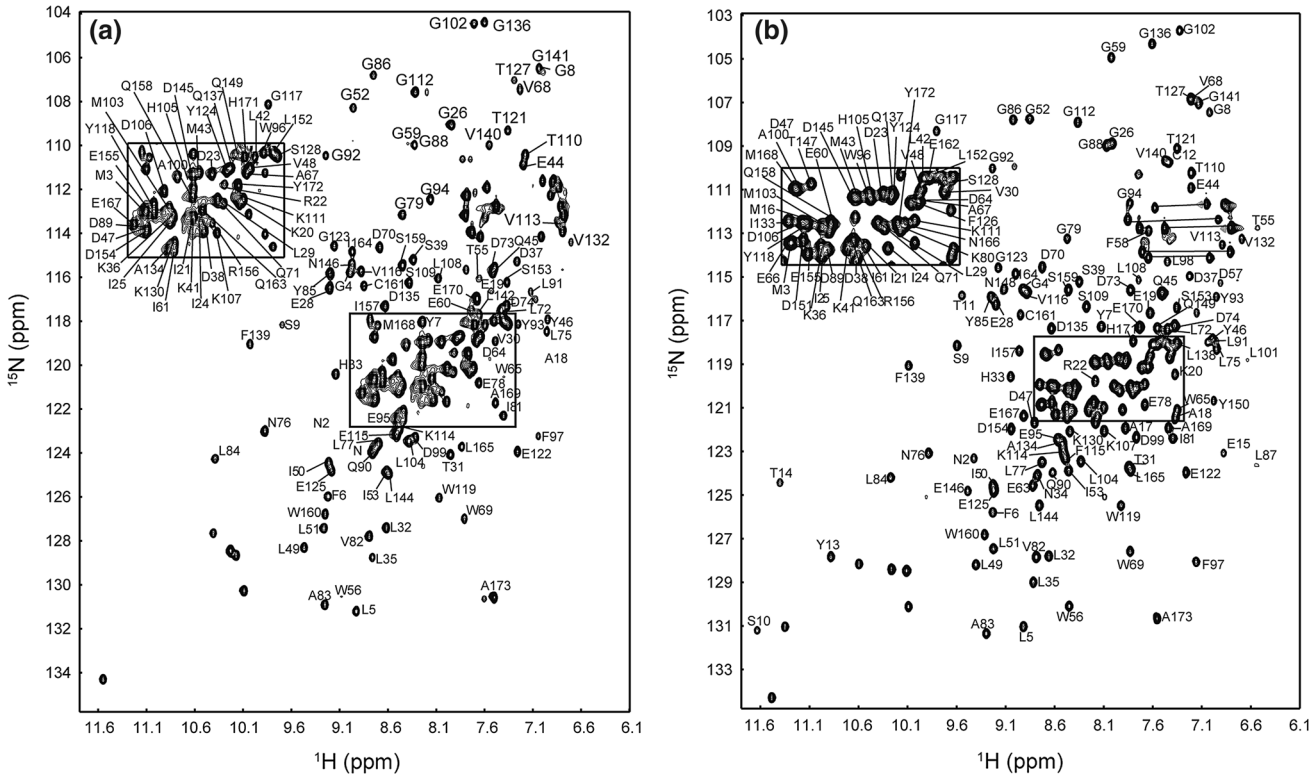

Fig. 1 Backbone assignments of apo- and holo-FldB. 2D ^{1}H–^{15}N HSQC spectra of *E. coli* FldB in its apo- (**a**) and holo-forms (**b**) with backbone assignments labeled with residue number and amino acid codes

COSY, and (H)CCH-TOCSY experiments were collected for chemical shift assignments. 3D ^{15}N- and ^{13}C-edited NOESY-HSQC spectra (mixing times 100 ms) were performed to confirm the assignments and generate inter-proton distance restraints. The ^{1}H chemical shifts were referenced to internal DSS, and ^{13}C and ^{15}N chemical shifts were referenced indirectly. All spectra were processed using the software package NMRPipe (Delaglio et al. 1995) and analyzed by the program NMRView (Johnson and Blevins 1994).

More than 96 and 90 % shift assignments were obtained for holo- and apo-FldB, respectively. For holo-FldB, the ^{15}N-HSQC spectrum was well dispersed and all backbone amide signals were assigned except for the N-terminal Met1. For apo-FldB, on the other hand, a total of 17 backbone amide signals were missing, all of which locate on the FMN binding P-loop or 50's loop (Fig. 1). The assigned ^{1}H, ^{13}C and ^{15}N chemical shifts of the apo- and holo-FldB have been deposited in the BioMagResBank (http://www.bmrb.wisc.edu/) under the accession numbers 25155 and 25153, respectively.

Structure calculations

The structures were calculated using the program CYANA (Güntert 2004) and refined with AMBER (Pearlman et al. 1995). Distance restraints were derived from inter-proton nuclear Overhauser effect (NOE). Dihedral angles (φ and ψ) were predicted from chemical shifts using TALOS (Cornilescu et al. 1999). 200 structures were first calculated by CYANA, and the 100 structures with the lowest target function values were selected and further refined by AMBER. Finally, 20 lowest-energy conformers were selected as the representative structures. In the structure calculation of holo-FldB, in addition to intermolecular NOEs identified between the protein and the FMN molecule, distance restraints were also added between the phosphate group of the FMN molecule and residues in the P-loop based on their significant chemical shift perturbations (Barsukov et al. 1997). The structural statistics are summarized in Table 1, and the atomic coordinates of apo- and holo-FldB have been deposited in the Protein Data Bank (PDB) under the accession codes 2mtb and 2mt9, respectively.

Relaxation measurements

The backbone ^{15}N relaxation parameters, including the longitudinal relaxation rates (R_1), transverse relaxation rates (R_2), and steady-state heteronuclear $\{^{1}H\}$–^{15}N NOE values of the apo- and holo-FldB were measured on a Bruker Avance 800 MHz NMR spectrometer at 25 °C. All experiments were carried out using conventional HSQC scheme similar to previously described (Barbato et al. 1992; Farrow et al. 1994) but with water flip-back for solvent suppression (Chen and Tjandra 2011). Recycle delays were set to 3 s for R_1 and R_2 experiments. The $\{^{1}H\}$–^{15}N NOE experiments were performed in the presence and absence of a 3-s proton presaturation period prior to the ^{15}N excitation pulse and using recycle delays of 2 and 5 s, respectively (Markley et al. 1971; Renner et al. 2002). The delays used for the R_1 experiments were 10 (×2), 100 (×2), 300, 600, 800, 1,000, 1,600, 2,400, 3,200, 4,000 and 5,000 ms. The delays used for the R_2 experiments were 7.4 (×2), 14.8, 22.3, 37.1, 29.7, 52.0, 66.8, 89.1, 111.4 and 141.1 ms. The relaxation rate constants were obtained by fitting the peak intensities to a single exponential function using the nonlinear least squares method as described (Fushman et al. 1997), and the relaxation data were analyzed using the Model-free formalism (Lipari and Szabo 1982a, b; Clore et al. 1990).

Table 1 Structural statistics of *E. coli* FldB

	Apo-FldB	Holo-FldB
Structural restraints		
Protein intramolecular NOEs		
Total unambiguous NOEs	4,237	5,885
Intra-residue	1,917	2,386
Sequential ($\|i - j\| = 1$)	939	1,387
Medium-range ($1 < \|i - j\| < 5$)	479	708
Long-range	902	1,404
Total ambiguous NOEs	1,036	1,526
Protein-FMN intermolecular distance restraints	–	9
Dihedral angle restraints ($\phi + \psi$)	224 (112 + 112)	226 (113 + 113)
Restraint violations		
Distance (>0.3 Å)	0	0
Dihedral angle (>5°)	0	0
r.m.s.d. from mean structure (Å)		
Secondary structure backbone atoms	0.31 ± 0.07	0.20 ± 0.03
Secondary structure heavy atoms	0.33 ± 0.07	0.27 ± 0.04
All backbone atoms	0.85 ± 0.10	0.30 ± 0.05
All heavy atoms	0.89 ± 0.11	0.33 ± 0.05
Ramachandran statistics (%)		
Residues in most favored regions	88.0	88.7
Residues in additional allowed regions	10.0	9.1
Residues in generously allowed regions	1.3	1.5
Residues in disallowed regions	0.7	0.7

Discussion and conclusions

Solution structures of apo- and holo-FldB

FldB shows a typical flavodoxin fold consisting an α/β sandwich with a central five-strand parallel β-sheet (β1: Met3-Tyr7, β2: Val30-Asn34, β3: Val48-Leu51, β4: Ile81-Leu87, β5: Lys114-Val116 and Leu142-Leu144) flanked by five α-helices (α1: Ile17-Ile25, α2: Pro40-Glu44, α3: Glu63-Leu72, α4: Asp99-Ser109, α5: Asp151-Glu172) on two sides (Fig. 2a, b). The β5 was split in the middle by a 20-residue insertion (Pro120-Gly141) which is unique to the long-chain flavodoxin subfamily. This extra sequence forms an additional small three-strand β-sheet (β1*: Trp119-Pro120, β2*: Val132-Ile133, β3*: Leu138-Phe139) and protrudes on one side of the structure. The FMN-binding site is formed by three active loops, namely the P-loop (Gly8-Met16), the 50's loop (Gly52-Gln62) and the 90's loop (Gly88-Leu98). The P-loop is responsible for binding the phosphate group, whereas the 50s and 90s loops together bind the aromatic flavin ring of the FMN molecule. Residues Thr121-Pro131 in the insertion sequence form a relatively long loop (termed the 'extra loop' hereafter), which is packed close to the outside of the 90s loop but does not directly involve in FMN binding.

Comparison of apo- and holo-FldB structures shows an essentially identical structure core (Fig. 3), with a root mean square deviation 0.94 Å for backbone Cα atoms. The most significant conformational difference between these two forms is observed at the FMN-binding loops. These loops are well defined in the holo-form, whereas they are highly mobile and adopt flexible conformations in the apo-form as indicated by the missing of backbone amide signals and the lack of NOE contacts. Moreover, we observed

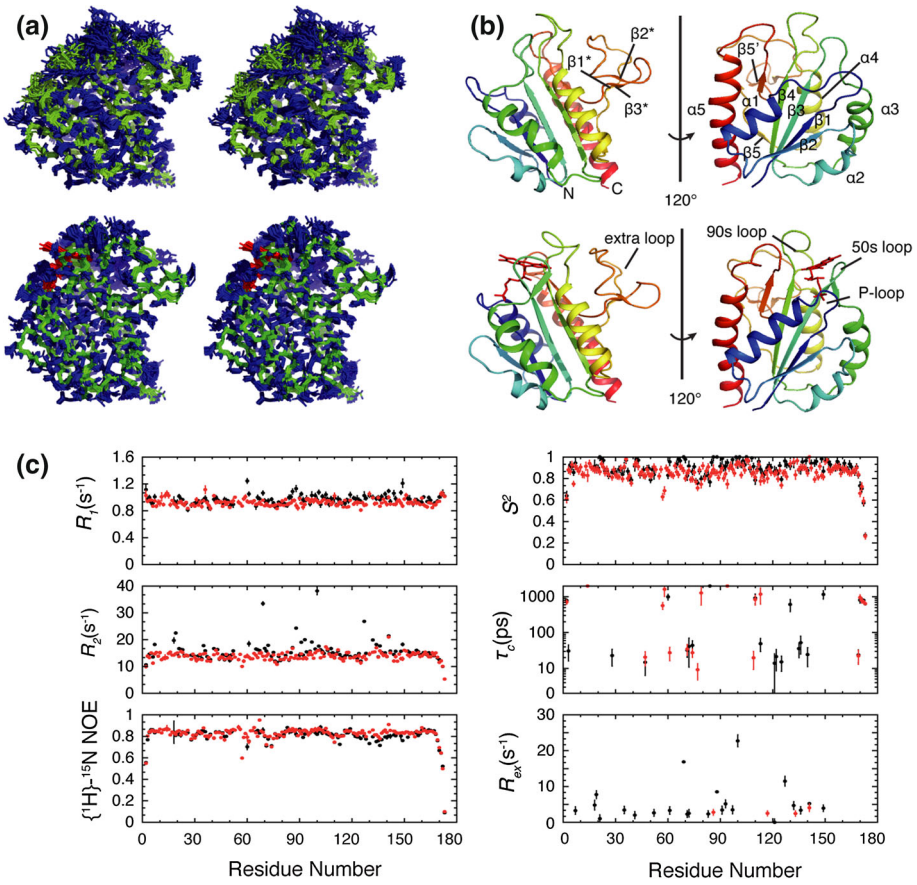

Fig. 2 Solution structures and backbone dynamics of apo- and holo-FldB. **a** Superimposition of 20 representative solution structures of apo- and holo-FldB in stereo. Main chain and converged side chains are colored in *green* and *blue*, respectively. The side chains of residues Ser10-Ala17, Asp57-Tyr58, Gln62-Glu63, Leu98, Ala143, Glu146-Thr147 and Tyr150 in apo-FldB are not shown since they have no backbone assignment or few NOE contacts. **b** Ribbon diagram representation of apo and holo-FldB, with secondary structural elements and loops labeled. The FMN molecule is shown in *red*. **c** Backbone relaxation data and internal dynamic parameters of apo- and holo-FldB shown in *black* and *red*, respectively. The relaxation data of the longitudinal relaxation rates R_1, transverse relaxation rates R_2, and heteronuclear $\{^1H\}$–^{15}N NOE were recorded on a Bruker Avance 800-MHz spectrometer at 25 °C. The microscopic dynamic parameters S^2, τ_e, and R_{ex} were extracted from Model-free analyses

secondary structure extension in the holo-form. In particular, helix α1 extends four residues at the N-terminal end towards the FMN-binding pocket upon FMN binding. The stabilization of FldB structure upon FMN binding is also supported by backbone ^{15}N dynamics (Fig. 2c). Relaxation parameters and model-free analysis identified many residues around the FMN binding loops exhibit significant conformational exchanges on the μs-ms timescales in the apo-form, whereas only a few residues (Gly86, Gly117, Ile133 and Gly141) show conformational exchanges on the slow timescales.

Structural comparison with *E. coli* FldA

The amino acid sequences of *E. coli* FldB and FldA share 40.8 % identity and 61.5 % similarity, and a structure overlay of the two in holo-forms showed an r.m.s.d value of 1.0 Å for the aligned Cα atoms. A detailed comparison of amino acid composition differences at the FMN binding loops as well as the extra loop region is shown in Fig. 3. In the phosphate-binding P-loop, a negatively charged Asp11 in FldA is replaced by Ser10 in FldB, a flexible Gly13-Asn14 dipeptide in FldA is substituted by the Cys12-Tyr13 sequence in FldB bearing the hydrophobic and bulky aromatic side chain. The 50s loop region is relatively conserved between the two proteins, except that the aromatic Tyr58 in FldA is replaced by an acidic Asp57 in FldB. In addition, two acidic residues Glu92-Asp93 in the 90s loop of FldA is replaced by Leu91-Gly92 in FldB. It has been proposed that negative charges and aromatic rings near the flavin ring may contribute to the lowering of the E1 potential, which corresponds to the transition between the sq and hq states (Hoover and Ludwig 1997; McCarthy et al. 2002; Alagaratnam et al. 2005). Though the exact affect caused by the amino acid difference in the P-loop remains to be investigated, the decreased number of aromatic and negatively charged residues in the 50s and 90s loop in FldB may modulate its redox potentials and thus affecting its biological roles. On the other hand, the FldA and FldB proteins also show different distribution of charged residues on the extra loop, which is believed to play a role in protein partner recognition, and thus may also define the divergent functions of the two closely related flavodoxins in vivo.

Intriguingly, although the sequence conservation is relatively high at the 50s loop for the two proteins, we observed a considerable difference in their dynamic behaviors in the holo-forms. In holo-FldA, certain residues in the 50s loop exhibit conformational exchanges on the μs–ms timescales (Ye et al. 2014). The phenomenon is similarly observed in several other flavodoxins and may be related to the local backbone flip during redox reactions (Hu et al. 2006; Ye et al. 2014; Hrovat et al. 1997). In contrast, the holo-FldB protein is generally rigid and no conformational exchanges were observed in the 50s loop region, which is similar to a previous backbone ^{15}N

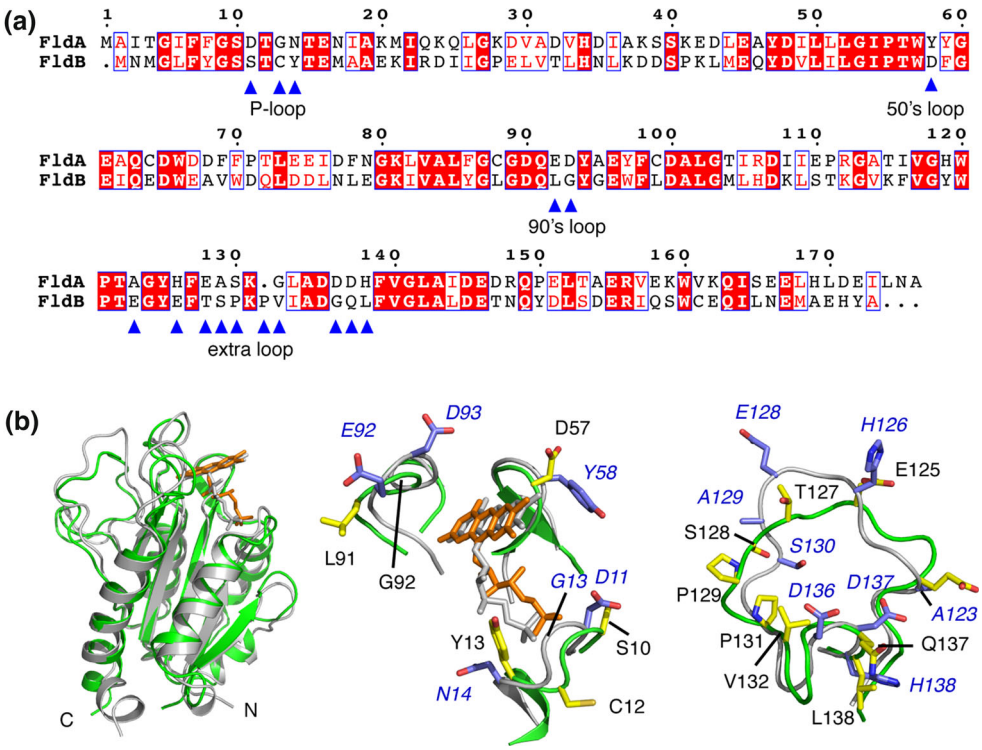

Fig. 3 Sequence and structural comparison between *E. coli* FldA and FldB. **a** Sequence alignment of the *E. coli* FldA and FldB proteins. Major differences in the FMN-binding loops and the extra loop are indicated by *blue triangles*. **b** The *left* panel shows an overlay of the structures of FldB (*green*) with FldA (*grey*). The *middle* and *right* panels show the local structural differences at the FMN-binding loops and the extra loops region. The major amino acid differences as labeled in (**a**) are depicted on the structures

relaxation study of the *Anacystis nidulans* flavodoxin (Zhang et al. 1997). In addition, although the experimental conditions and pulse scheme used were similar, the measured R_1 values for FldB are slightly higher than those of FldA. The average R_1 value for rigid residues is 0.87 ± 0.04 for holo-FldA and 0.92 ± 0.05 for holo-FldB, indicating difference of intrinsic dynamics between the two proteins. Whether or not the dynamic differences between FldA and FldB play a key role in differentiating their functions remains to be further investigated.

Acknowledgments All NMR experiments were performed at the Beijing NMR Center and the NMR facility of National Center for Protein Sciences at Peking University. This research was supported by Grant 31100525 from the National Natural Science Foundation of China to Y.H.

References

Alagaratnam S, van Pouderoyen G, Pijning T, Dijkstra BW, Cavazzini D, Rossi GL, Van Dongen WM, van Mierlo CP, van Berkel WJ, Canters GW (2005) A crystallographic study of Cys69Ala flavodoxin II from *Azotobacter vinelandii*: structural determinants of redox potential. Protein Sci 14:2284–2295

Barbato G, Ikura M, Kay LE, Pastor RW, Bax A (1992) Backbone dynamics of calmodulin studied by N-15 relaxation using inverse detected 2-dimensional NMR-spectroscopy—the central helix is flexible. Biochemistry 31:5269–5278

Barsukov I, Modi S, Lian LY, Sze KH, Paine MJ, Wolf CR, Roberts GC (1997) ^{1}H, ^{15}N and ^{13}C NMR resonance assignment, secondary structure and global fold of the FMN-binding domain of human cytochrome P450 reductase. J Biomol NMR 10:63–75

Chen K, Tjandra N (2011) Water proton spin saturation affects measured protein backbone ^{15}N spin relaxation rates. J Magn Reson 213:151–157

Clore GM, Szabo A, Bax A, Kay LE, Driscoll PC, Gronenborn AM (1990) Deviations from the simple two-parameter model-free approach to the interpretation of N-15 nuclear magnetic-relaxation of proteins. J Am Chem Soc 112:4989–4991

Cornilescu G, Delaglio F, Bax A (1999) Protein backbone angle restraints from searching a database for chemical shift and sequence homology. J Biomol NMR 13:289–302

Delaglio F, Grzesiek S, Vuister GW, Zhu G, Pfeifer J, Bax A (1995) NMRPipe—a multidimensional spectral processing system based on Unix pipes. J Biomol NMR 6:277–293

Edmondson DE, Tollin G (1971) Chemical and physical characterization of the *Shethna* flavoprotein and apoprotein and kinetics and thermodynamics of flavin analog binding to the apoprotein. Biochemistry 10:124–132

Farrow NA, Muhandiram R, Singer AU, Pascal SM, Kay CM, Gish G, Shoelson SE, Pawson T, Forman-Kay JD, Kay LE (1994) Backbone dynamics of a free and phosphopeptide-complexed Src homology 2 domain studied by ^{15}N NMR relaxation. Biochemistry 33:5984–6003

Fushman D, Cahill S, Cowburn D (1997) The main-chain dynamics of the dynamin pleckstrin homology (PH) domain in solution: analysis of 15N relaxation with monomer/dimer equilibration. J Mol Biol 266:173–194

Gaudu P, Weiss B (2000) Flavodoxin mutants of *Escherichia coli* K-12. J Bacteriol 182:1788–1793

Güntert P (2004) Automated NMR structure calculation with CYANA. Methods Mol Biol 278:353–378

Hoover DM, Ludwig ML (1997) A flavodoxin that is required for enzyme activation: the structure of oxidized flavodoxin from *Escherichia coli* at 1.8 Å resolution. Protein Sci 6:2525–2537

Hrovat A, Blumel M, Lohr F, Mayhew SG, Ruterjans H (1997) Backbone dynamics of oxidized and reduced *D. vulgaris* flavodoxin in solution. J Biomol NMR 10:53–62

Hu Y, Li Y, Zhang X, Guo X, Xia B, Jin C (2006) Solution structures and backbone dynamics of a flavodoxin MioC from *Escherichia coli* in both apo- and holo-forms: implications for cofactor binding and electron transfer. J Biol Chem 281:35454–35466

Johnson BA, Blevins RA (1994) NMRView: a computer program for the visualization and analysis of NMR data. J Biomol NMR 4:603–614

Knight EJ, Hardy RW (1967) Flavodoxin. Chemical and biological properties. J Biol Chem 7:1370–1374

Lipari G, Szabo A (1982a) Model-free approach to the interpretation of nuclear magnetic resonance relaxation in macromolecules. 1. Theory and range of validity. J Am Chem Soc 104:4546–4559

Lipari G, Szabo A (1982b) Model-free approach to the interpretation of nuclear magnetic resonance relaxation in macromolecules. 2. Analysis of experimental results. J Am Chem Soc 104:4559–4570

López-Llano J, Maldonado S, Bueno M, Lostao A, Angeles-Jiménez M, Lillo MP, Sancho J (2004a) The long and short flavodoxins: I. the role of the differentiating loop in apoflavodoxin structure and FMN binding. J Biol Chem 45:47177–47183

López-Llano J, Maldonado S, Jain S, Lostao A, Godoy-Ruiz R, Sanchez-Ruiz JM, Cortijo M, Fernández-Recio J, Sancho J (2004b) The long and short flavodoxins: II. the role of the differentiating loop in apoflavodoxin stability and folding mechanism. J Biol Chem 45:47184–47191

Markley LJ, Horsley WJ, Klein MP (1971) Spin-lattice relaxation measurements in slowly relaxing complex spectra. J Chem Phys 55:3604–3605

Marley J, Lu M, Bracken C (2001) A method for efficient isotopic labeling of recombinant proteins. J Biomol NMR 20:71–75

McCarthy AA, Walsh MA, Verma CS, O'Connell DP, Reinhold M, Yalloway GN, D'Arcy D, Higgins TM, Voordouw G, Mayhew SG (2002) Crystallographic investigation of the role of aspartate 95 in the modulation of the redox potentials of *Desulfovibrio vulgaris* flavodoxin. Biochemistry 41:10950–10962

Pearlman DA, Case DA, Caldwell JW, Ross WS, Cheatham TE, Debolt S, Ferguson D, Seibel G, Kollman P (1995) Amber, a package of computer-programs for applying molecular mechanics, normal-mode analysis, molecular-dynamics and free-energy calculations to simulate the structural and energetic properties of molecules. Comput Phys Commun 91:1–41

Renner C, Schleicher M, Moroder L, Holak TA (2002) Practical aspects of the 2D ^{15}N–{^{1}H}–NOE experiment. J Biomol NMR 23:23–33

Sancho J (2006) Flavodoxins: sequence, folding, binding, function and beyond. Cell Mol Life Sci 63:855–864

Ye Q, Hu Y, Jin C (2014) Conformational dynamics of *Escherichia coli* flavodoxins in apo- and holo-states by solution NMR spectroscopy. PLoS One 9:e103936

Zhang P, Dayie KT, Wagner G (1997) Unusual lack of internal mobility and fast overall tumbling in oxidized flavodoxin from *Anacystis nidulans*. J Mol Biol 272:443–455